Original Article

Polysaccharide from *Schisandra chinensis* alleviates ulcerative colitis by improving intestinal microbiota abundance and inhibiting the TLR4/p65/IκBα pathway in Dextran sodium sulfate-induced mice

Caihong Wu[1*] Yang Yang[1] Peng Liu[1] Bin Zhang[1] Hui Lu[1]

Abstract

Schisandra chinensis polysaccharides (SCP) are isolated from *Schisandra chinensis* with a mean molecular weight of 32.401 kDa. Previous studies have demonstrated that *Schisandra chinensis* extract effectively prevented colitis and modulated gut microbiota in dextran sulfate sodium (DSS)-induced mice. In this study, 3% DSS was used to induce acute ulcerative colitis in mice, and then the SCP with different doses (50 mg/kg, 100 mg/kg, 200 mg/kg) and 5-aminosalicylic acid (5-ASA) were used to treat mice by oral gavage for one week. Here, we report for the first time that SCP presents outstanding protective effects on colon damage induced by DSS in mice. Firstly, SCP decreased oxidative stress, downregulated the expression of inflammatory factors, and inhibited the TLR4/p65/IκBα pathway in the colon. Then, SCP reversed DSS-induced intestinal barrier damage by improving the tight junction proteins. Moreover, SCP improved the levels of SCFA in the intestine of mice. Furthermore, SCP increased the diversity of gut microbiota and the abundance of beneficial bacteria, especially *Lactobacillus* and *Akkermansia*. Our results indicated that the protective effect of SCP on colitis caused by DSS may be due to inhibiting the TLR4/p65/IκBα pathway and the regulation of gut microbiota.

Keywords: gut microbiota, *Schisandra chinensis* polysaccharides, TLR4/p65/IκBα pathway

[1]*College of Veterinary Medicine, Jiangsu Agri-animal Husbandry Vocational College, Taizhou, Jiangsu 225300, China*
***Correspondence**: caihongwu616@aliyun.com* (Caihong Wu)
Received May 27, 2025
Accepted September 17, 2025
https://doi.org/10.56808/2985-1130.3872

Introduction

Ulcerative colitis (UC) is a chronic inflammatory bowel disease characterized by inflammation and ulceration of the colonic mucosa. The etiology of UC involves a complex interplay of genetic, environmental, and immunological factors (Kobayashi *et al*., 2020; Schlegel *et al*., 2021). The severity of colitis can be assessed using the disease activity index (DAI), histological analysis, and cytokine secretion measurements (Wen *et al*., 2013; Xiao *et al*., 2022). Dextran sodium sulfate (DSS)-induced colitis model in mice has been widely used to study UC due to its similarities to the human disease (Gobert *et al*., 2022). Understanding the mechanisms and therapeutic interventions in DSS-induced colitis can contribute to the development of effective strategies for managing UC in humans.

Toll-like receptor 4 (TLR4) is a key receptor involved in recognizing microbial components and initiating the immune response. Upon activation by DSS, TLR4 triggers downstream signaling through the p65 subunit of NF-κB, resulting in the activation of pro-inflammatory cytokines and chemokines (Zhang *et al*., 2022). Several studies have demonstrated the crucial role of the TLR4/p65 pathway in the pathogenesis of DSS-induced colitis (Shi *et al*., 2019; Xue *et al*., 2019). production of pro-inflammatory cytokines, such as tumor necrosis factor-alpha (TNF-α) and interleukin-6 (IL-6), which contribute to the development and progression of colitis (Mei *et al*., 2022). Inhibition of the TLR4/p65 pathway has shown promising therapeutic effects in DSS-induced colitis (Xue *et al*., 2019; Yan *et al*., 2022). Therefore, targeting the TLR4/p65 pathway may hold therapeutic potential for treating DSS-induced colitis.

The intestinal barrier is the first and key line of defense against harmful bacteria, toxins, and pathogens, crucial for protecting the host's health (Spencer and Bemark, 2023). The gut microbiota's abundance affects the intestinal barrier function and the physiological function of extraintestinal organs (Glorieux *et al*., 2023). Dysbiosis, characterized by an imbalance in the composition and diversity of the gut microbiota, has been implicated in the pathogenesis of DSS-induced colitis. Several studies have shown alterations in the gut microbiota composition and function in this model (Lu *et al*., 2023; Yang *et al*., 2023a). Dysbiosis leads to a disrupted intestinal barrier, increased mucosal permeability, and immune activation, ultimately contributing to the development and progression of colitis (Sinha *et al*., 2020). Modulating the gut microbiota has emerged as a potential therapeutic approach for DSS-induced colitis. Probiotics, prebiotics, and postbiotics have been investigated for their ability to restore gut microbial balance and ameliorate colitis severity (Shi *et al*., 2020). These interventions have shown promising results in attenuating inflammation, improving gut barrier function, and modulating immune responses in DSS-induced colitis. Furthermore, specific bacterial strains, such as Bifidobacterium and Lactobacillus species, have been found to exert protective effects in this model (Liu *et al*., 2023; Wu *et al*., 2023).

Polysaccharides are complex macromolecules that are non-toxic, affordable, and have strong activity, making them ideal for use in the food and pharmaceutical industries (Mukherjee *et al*., 2022). Naturally derived polysaccharides exhibit a wide range of beneficial effects, including immunomodulation, anti-oxidation, and anti-inflammation (Li *et al*., 2018; Mukherjee *et al*., 2022). Their mechanisms often involve the regulation of immune cell functions, scavenging of reactive oxygen species, and the protection of intestinal mucosal barriers (Mei *et al*., 2022; Yang *et al*., 2023). Furthermore, many plant polysaccharides serve as prebiotics, selectively promoting the growth of beneficial gut bacteria such as *Lactobacillus* and *Bifidobacterium*, which is crucial for maintaining gut homeostasis and alleviating colitis (Su *et al*., 2020; Lu *et al*., 2023). *Schisandra chinensis*, a traditional Chinese medicinal herb commonly known as Wu Wei Zi or Five-Flavor Berry, has been recognized for its diverse pharmacological properties. Studies have demonstrated that *Schisandra chinensis* (Turcz.) Baill can inhibit the TLR4/p65 pathway, thereby reducing inflammation in colitis (Bian *et al*., 2022). *Schisandra chinensis* polysaccharides (SCP) have been shown to possess anti-inflammatory, antioxidant, and immunomodulatory properties (Li *et al*., 2018; Su *et al*., 2020). Polysaccharides derived from *Schisandra chinensis* have gained attention for their potential therapeutic benefits in various diseases, including colitis (Su *et al*., 2020). Additionally, SCP have been found to modulate the composition and abundance of the gut microbiota, promoting a balanced microbial community (Fu *et al*., 2023). However, whether SCP could alleviate DSS-induced colitis by regulating the abundance of gut microbiota and TLR4/p65 pathway was still unclear.

In this study, we aimed to investigate the therapeutic potential of polysaccharides from *Schisandra chinensis* in DSS-induced colitis. We hypothesized that the SCP could alleviate colitis by improving the abundance of intestinal microbiota and inhibiting the TLR4/p65 pathway. To address this hypothesis, we established a DSS-induced colitis mouse model and evaluated the effects of polysaccharide treatment on colitis severity, intestinal microbiota composition, and TLR4/p65 pathway activation. Understanding the mechanisms underlying the beneficial effects of SCP in colitis could provide novel insights into the development of targeted therapies for UC. These results provide new insights into the health benefits of polysaccharides extracted from *Schisandra chinensis*.

Materials and Methods

Extraction and purification of Schisandra chinensis polysaccharides: *Schisandra chinensis* was purchased from Bozhou Hengyi Traditional Chinese Medicine Technology Co., Ltd. *Schisandra chinensis* polysaccharides (SCP) were isolated from the *Schisandra chinensis* as previously described (Yang *et al*., 2023b). Briefly, remove lipophilic components from *Schisandra chinensis* (1.0 kg) by refluxing anhydrous ethanol for 2 hours. After drying the collected *Schisandra chinensis*, the supernatant was extracted by

water extraction and alcohol precipitation, and the extracted solution was then diluted with 5000 × g for 10 min to obtain the crude product of SCP. Next, the protein in the crude polysaccharide was removed by Sevag (chloroform/n-butanol 4:1), and finally, SCP was obtained through freeze-drying.

SEM analysis of SCP: The microstructural features of SCP were observed by a field emission scanning electron microscope (SEM) Regulus 8100 system (Tokyo, Japan). The samples were coated with gold and detected with a 5 kV accelerating voltage.

Fourier transform-infrared (FT-IR) analysis of SCP: FT-IR was analyzed according to previously reported (Yang *et al*., 2023b). In brief, five milligrams of the SCP sample were mixed with 300 mg of potassium bromide and pressed into a 1mm thick sheet. The UV spectra of SCP were determined using FT-IR spectrometer (Nicolet iZ-10, USA) in the frequency range of 400-4000 cm-1 by Sanshu Biotech. Co., LTD (Shanghai, China).

Molecular weight analysis: The molecular weight of SCP was determined according to a previously reported (Yang *et al*., 2023b). Dissolve the SCP in a 0.1 M NaNO3 solution with a concentration of 1mg/mL and then filter through a filter (0.45 μm) before detection. Then the molecular weight of SCP was determined using a GPC-MALLS system.

Monosaccharide composition analysis of SCP: The monosaccharide composition of SCP was examined by high-performance anion-exchange chromatography (HPAEC) according to previous research (Yang *et al*., 2023b). In short, 5 mg of SCP was supplemented with 5 mL of 2 M TFA and then mixed at 121 ℃ for 4 h. The SCP was washed with methanol and then volatilized under nitrogen, repeated 3 times, then examined by HPAEC.

Animal experiment: Forty-eight ICR mice (6-week-old, male) were obtained from Yangzhou University (Yangzhou, China). This study was approved by the Ethics Committee of Animal Experiments Center of Jiangsu Agri-Animal Husbandry Vocational College (Approval Number jsahvc-2023-10). After adapting to the laboratory conditions, mice were separated into six groups as follows: 1) Control group (CON); 2) model group (DSS); 3) positive control group (5-ASA); 4) Low-dose SCP group (DSS+50 mg/kg SCP); 5) Medium-dose SCP group (DSS+100 mg/kg SCP); 6) High-dose SCP group (DSS+200 mg/kg SCP). The mice were housed for 3 weeks. The behavioral tests (8 mice per group) were performed at the end of the experiment, after which all the mice were sacrificed. Except for the control group, which was given pure water during the experiment, the other five groups were given 3% DSS solution orally for 7 days to establish the inflammatory colitis mouse model. The experiment groups administered different doses of SCP once a day, respectively. Mice in the positive group (5-ASA group) were intragastrically administered 5-aminosalicylic acid (200 mg/kg) (Shanghai Maclin Biochemical Co., LTD.). Other groups were intragastrically given 0.9% NaCl for 7 days. The DAI score was determined by weight loss, stool consistency, and blood in the stool. After the experiment, the mice were sacrificed by cervical dislocation after carbon dioxide absorption anesthesia. The Colon tissues were collected, and the length of the colon from the cecum to anus was measured and recorded. Cecum contents were collected and stored at -80 °C. Then, the colon tissue was washed with phosphate-buffered saline (PBS) and cut into two parts. One part was fixed with 4% paraformaldehyde for histological evaluation, and the other part was stored at -80 ℃ for subsequent study.

Histopathological analysis: Colon was fixed with 4% paraformaldehyde, and 4 μm sections of embedded tissues were cut and stained with hematoxylin and eosin (H&E) or periodic acid-schiff (PAS). The observation was made under optical microscopy at an appropriate magnification.

Analysis of biochemical parameters: The plasma concentrations of glucose, lactic dehydrogenase (LDH), triglyceride (TG), Total protein (TP), albumin (ALB), and globulin (GLOB) were measured by commercially available kits (Ningbo Meikang Biotechnology Co., Ltd, Zhejiang, China).

Analysis of inflammatory factors: The levels of tumor necrosis factor α (TNF-α, EK282), interleukin-6 (IL-6, EK206), and interleukin-1β (IL-1β, EK201B) in plasma, colon, duodenum, and jejunum were measured by ELISA kit (Multisciences Biotech, Hangzhou, China) according to the manufacturer's instructions.

Analysis of DAO, MDA, SOD, T-AOC activity: Diamine oxidase (DAO, A088-2-1) and Malondialdehyde (MDA, A003-1-2) levels, Superoxide dismutase (SOD, A001-3-2) and total antioxidant capacity (T-AOC, A015-2-1) activities were evaluated by commercially available kits (Nanjing Jiancheng Bioengineering Institute, Jiangsu, China).

Immunofluorescence staining: To determine the colonic levels of tight junction proteins, immunofluorescence staining was performed. Briefly, the histological sections were first deparaffinized and subjected to antigen retrieval, and then treated with PBS (0.1 M, pH 7.2) containing 5% goat serum to block nonspecific protein binding. After that, the colon sections were incubated with primary antibodies (ZO-1 and Occludin), and then ZO-1 and Occludin proteins were detected by fluorescence microscopy using the ZO-1-CY3 and Occludin-Alexa488 secondary antibodies in a Leica SP5 (Leica Microsystems, Wetzlar GmbH, Germany).

16S rRNA sequencing and analysis: Total genomic DNA from caecum contents was extracted by the CTAB method following a previous report (Wang *et al*., 2022). Total bacterial DNA was extracted from the fecal samples using the QIAamp DNA stool minikit (Qiagen, Hilden, Germany). Illumina NovaSeq sequencing analysis was performed by Genesky Biotechnologies, Inc. (Shanghai, China). 16S ribosomal RNA (16S rRNA) genes in the hypervariable region

(V3-V4 region) were amplified using specific primers. All PCR reactions were conducted using the Phusion® High-Fidelity PCR Master Mix (New England Biolabs). The PCR products were mixed in equidensity ratios, separated by gel electrophoresis, and purified with a gel extraction kit (Qiagen, Germany). The sequencing library was built up using the TruSeq® DNA PCR-free sample preparation kit (Illumina, USA) with reference to the manufacturer's instructions. Lastly, the library was sequenced on an Illumina NovaSeq platform to generate 250 bp paired-end reads. The compositional alteration of the gut microbiota at different taxonomic levels was analyzed using the Metastats method. Bioinformatics analyses of microbial data were performed by Genesky Biotechnologies, Inc.

RNA isolation and RT-PCR: Total RNA of the mouse colon was isolated using TRizol reagents (TSP401, Tsingke Biotechnology Co., Ltd, China). The procedure of RT-PCR, according to a previous study (Yang *et al*., 2021). The primers (Table 1) were synthesized by Tsingke Biotechnology Co., Ltd (Nanjing, Jiangsu, China).

Protein extraction and Western blotting: Colon protein was acquired by RIPA, and the concentration was detected with Bradford Protein Assay Kit (PC0010, Solarbio, China). Western blotting was performed according to a previous study (Yang *et al*., 2021). The antibody information for Western blot analysis is shown in Table 2.

Statistical analysis: Statistical analyses of data were performed using GraphPad Prism 8.0 (GraphPad Software, USA) and SPSS 20.0 (IBM, Armonk, NY), and data were presented as means ± SEM. The differences were analyzed using t-test or 2-way analysis. The differences were considered statistically significant when $P<0.05$.

Table 1 Nucleotide sequences of specific primers.

Target genes		Primer sequences (5′ to 3′)	GenBank accession
Tlr4	F: GCAAAGTCCCTGATGACATTCC	R: GGTGGTGTAAGCCATGCCA	NM_021297.3
p65	F: CAAGTGGCCATTGTGTTCCG	R: TGGCGATCATCTGTGTCTGG	NM_009045.4
Ikba	F: TTTGCCACTTTCCACTTAT	R: AATCCTGACCTGGTTTCG	NM_010907.2
Zo-1	F: ACCTCTGCAGCAATAAAGCAG	R: GAAATCGTGCTGATGTGCCA	XM_036152893.1
Occludin	F: TTCAGGTGAATGGGTCACCG	R: AGATAAGCGAACCTGCCGAG	NM_001360536.1
Tnfa	F: ATGTCTCAGCCTCTTCTCATTC	R: GCTTGTCACTCGAATTTTGAGA	NM_013693.3
Il-6	F: TTCTTGGGACTGATGCTGGT	R: AGACAGGTCTGTTGGGAGTG	NM_001314054.1
Il-1β	F: CTTACTGACTGGCATGAGGATCA	R: GCAGCTCTAGGAGCATGTGG	NM_010548.2
PPIA	F: GCAAGACCAGCAAGAAGA	R: CAGTGAGAGCAGAGATTACA	NM_008907

Table 2 Antibody information for Western blotting.

Antibody	Cat. Number	Company	Dilution ratioion
TLR4	66350-1-Ig	Proteintech	1:1000
P65	8242	Cell Signaling Technology	1:1000
p-P65	3033	Cell Signaling Technology	1:1000
IκBα	AF6239	Affinity	1:500
p-IκBα	AF3239	Affinity	1:1000
ZO-1	21773-1-AP	Proteintech	1:1000
Occludin	27260-1-AP	Proteintech	1:500
β-actin	AP0060	Bioworld	1:10,000

Results

Purification and characterization of SCP: The morphological characteristics of *Schisandra chinensis* polysaccharide were measured using SEM at magnifications of × 500 (Fig. 1A) and × 5 K (Fig. 1B), which showed irregular slices. The FT-IR spectra of SCP demonstrated typical absorption peaks of carbohydrate polymers (Fig. 1C). The stretching vibration absorption peak of -OH in the absorption band of 3600-3200 cm-1 is considered a characteristic peak of sugars.

In this study, a broad peak at 3388.72 cm-1, a characteristic peak of sugars, was ascribed to the stretching of the O-H group. The peak at 2938.00 cm−1 was assigned to the stretching vibrations of C-H groups. The peak at 1735.66 cm−1 was attributable to the stretching vibrations of C=O groups. The peaks at 1103.88 and 1017.98 cm−1 were attributable to the stretching vibrations of C-O groups. The average molecular weight (Mw) and number molar masses (Mn) were closely related to its biological activities and functions (Liu *et al*., 2020). In this study, GPC-MALLS results presented that the Mw and Mn of SCP were 32.401 kDa and 18.155 kDa, respectively (Fig. 1D). The monosaccharide composition of SCP was analyzed by HPAEC. The results showed that SCP consisted of rhamnose, arabinose, galactose, glucose, glucuronic acid, and had the molar proportion of 8.26:11.96:8.83:45.91:25.04 (Figs. 1E and 1F).

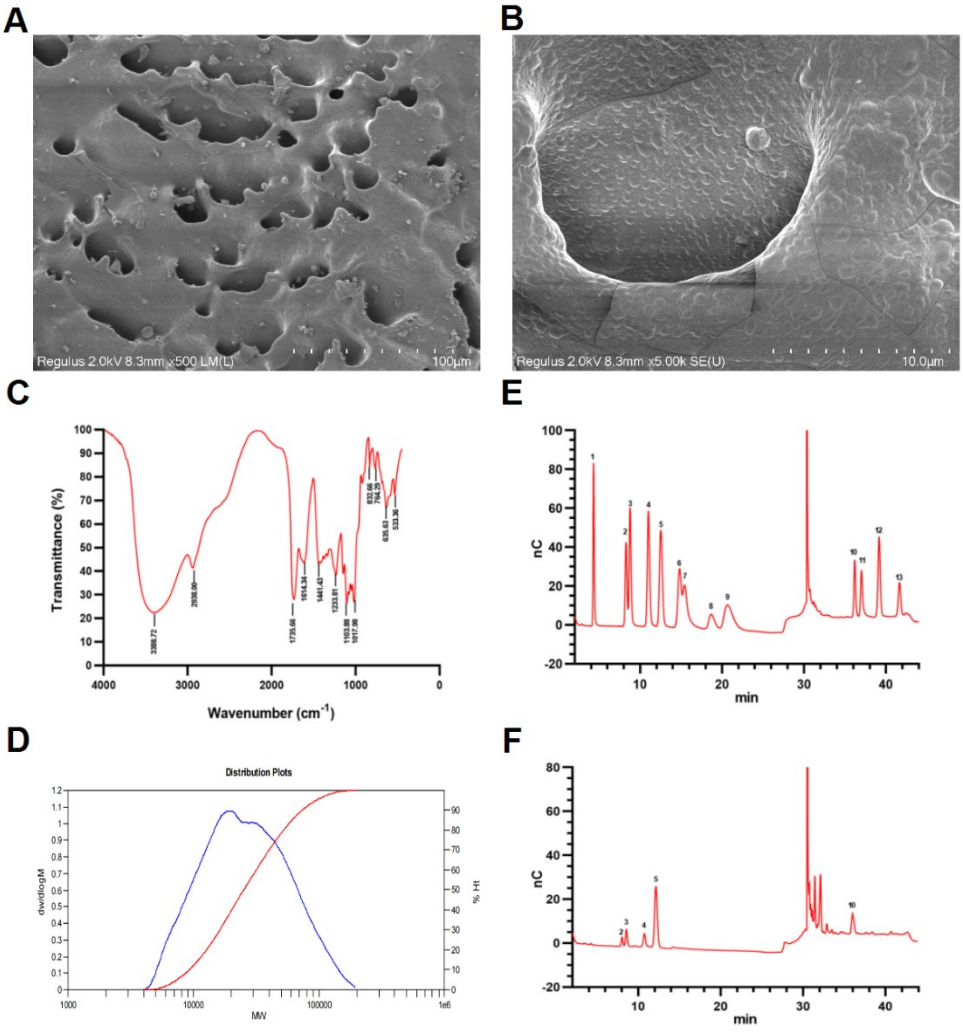

Figure 1 Extraction of polysaccharides from *Schisandra chinensis* (SCP) and physicochemical characteristics of purified polysaccharides (A-B) SEM images of SCP. (C) Fourier transforms infrared (FTIR) spectra of SCP; (D) GPC-MALLS elution patterns of the molecular weight distribution of SCP. (E-F) Monosaccharide composition of a standard mixture and SCP. (1, Fuc, fucose; 2, Rha, rhamnose; 3, Ara, arabinose; 4, Gal, galactose; 5, Glc, glucose; 6, Xyl, xylose; 7, Man, mannose; 8, Fru, Fructose; 9, Rib, Ribose; 10, Gal-UA, Galacturonic acid; 11, Gul-UA, Guluronic acid; 12, Glc-UA, Glucuronic acid; 13, Man-UA, Mannuronic acid).

The effect of SCP on body weight, colon length, and DAI score in DSS-treated mice: In this study, after seven-day oral administration of DSS, the body weight decreased significantly compared to that of the CON group (P<0.01). However, compared with DSS group, weight loss was significantly reversed after treatment with 5-ASA, M-SCP, and H-SCP (Fig. 2A). In addition, compared with the CON group, the colon length (Figs. 2B and 2C) was significantly decreased (P<0.01) in the DSS group, while the DAI score (Fig. 2D) was significantly increased. However, SCP dose-dependently inhibited colonic shortening in colitis mice, and the DAI score was significantly reduced (P<0.05). In addition, DSS treatment did not influence serum Glu level, while significantly increased (P<0.01) serum TG and LDH levels, as well as decreased (P<0.01) serum TP, ALB and GLOB levels, which was significantly reversed (P<0.05) by SCP and 5-ASA supplementation (Fig. 3).

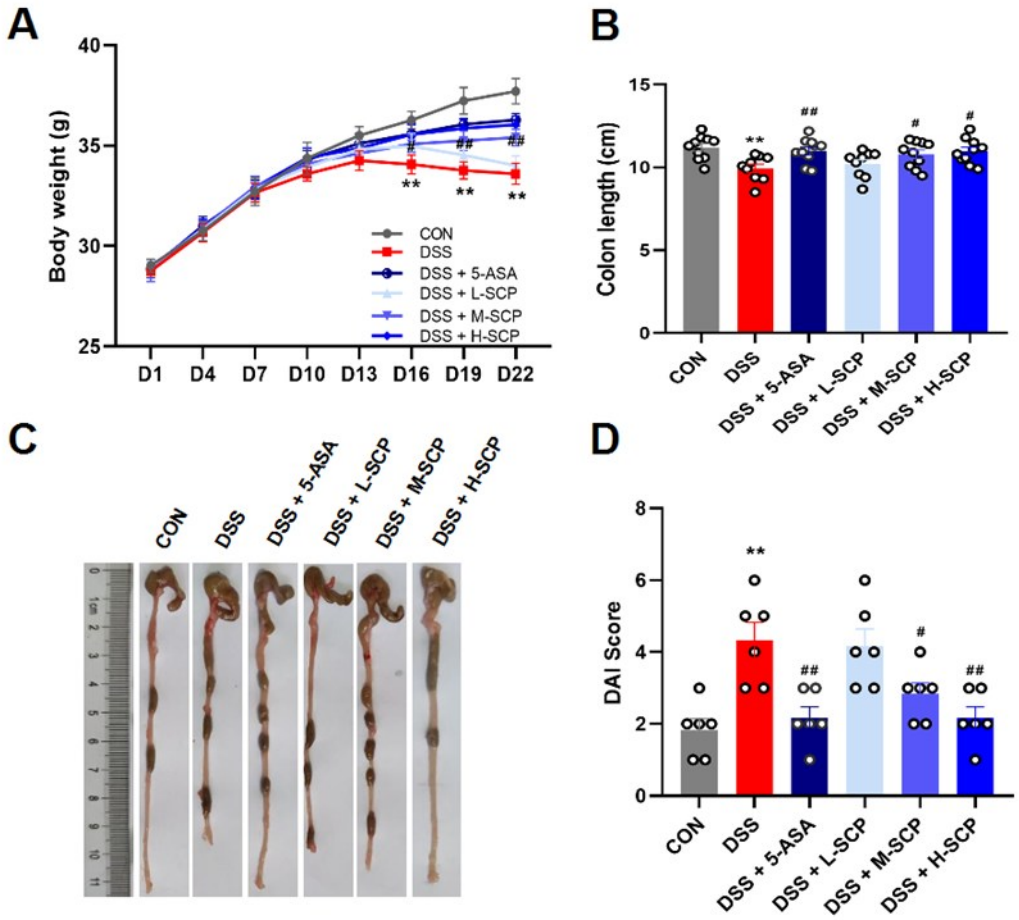

Figure 2 Effect of SCP on body weight and colon length in DSS-induced mice. (A) Daily Body weight changes during the experiment. (B) quantitative analysis of colon length in each group. (C) Representative photo of the colon in each group. (D) Disease activity index (DAI). Data are expressed as means ± SEM; n=6 for each group. **P*<0.05, ***P*<0.01 compare with CON group; #*P*<0.05, ##*P*<0.01 compare with DSS group.

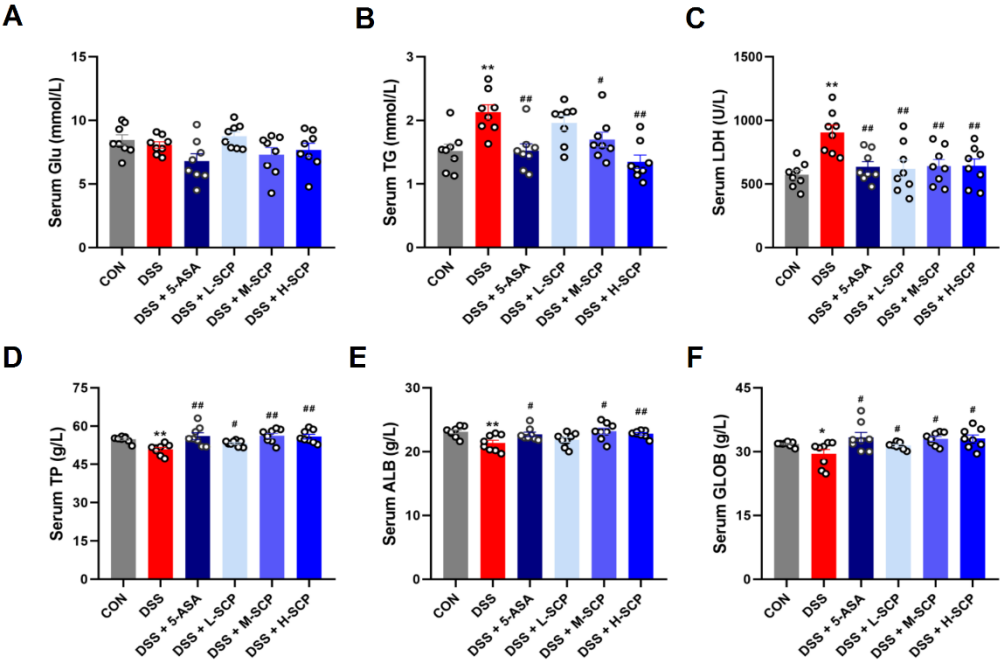

Figure 3 Effect of SCP on blood biochemical indices in DSS-induced mice. (A) Serum GLU level. (B) Serum TG level. (C) Serum LDH level. (D) Serum TP level. (E) Serum ALB level. (F) Serum GLOB level. Data are expressed as means±SEM; n=6 for each group. ***P*<0.01 compared with CON group; # *P*< 0.05, ##*P*<0.01 compare with DSS group.

The effect of SCP on inflammatory factors levels in serum and colon of DSS-treated mice: Inflammatory cytokine storm is a typical feature of UC pathogenesis. To further assess the effects of SCP on colonic inflammation, the ELISA and RT-qPCR were performed, respectively. Compared with the CON group, serum pro-inflammatory cytokines TNF-α (Fig. 4A), IL-6 (Fig. 4B), and IL-1β (Fig. 4C) levels were significantly increased (P<0.01) in the DSS group. While SCP and 5-ASA supplementation significantly decreased the concentrations of pro-inflammatory cytokines. In addition, the expression of colon TNF-α (Fig. 4D), IL-6 (Fig. 4E), and IL-1β (Fig. 4F) mRNA was significantly increased (P<0.01) in the DSS group, which was significantly reversed (P<0.01) by SCP and 5-ASA supplementation. Furthermore, colon TNF-α (Fig. 4G), IL-6 (Fig. 4H), and IL-1β (Fig. 4I) levels were significantly increased (P<0.01) in the DSS group, which were significantly reversed (P<0.01) by SCP and 5-ASA supplementation.

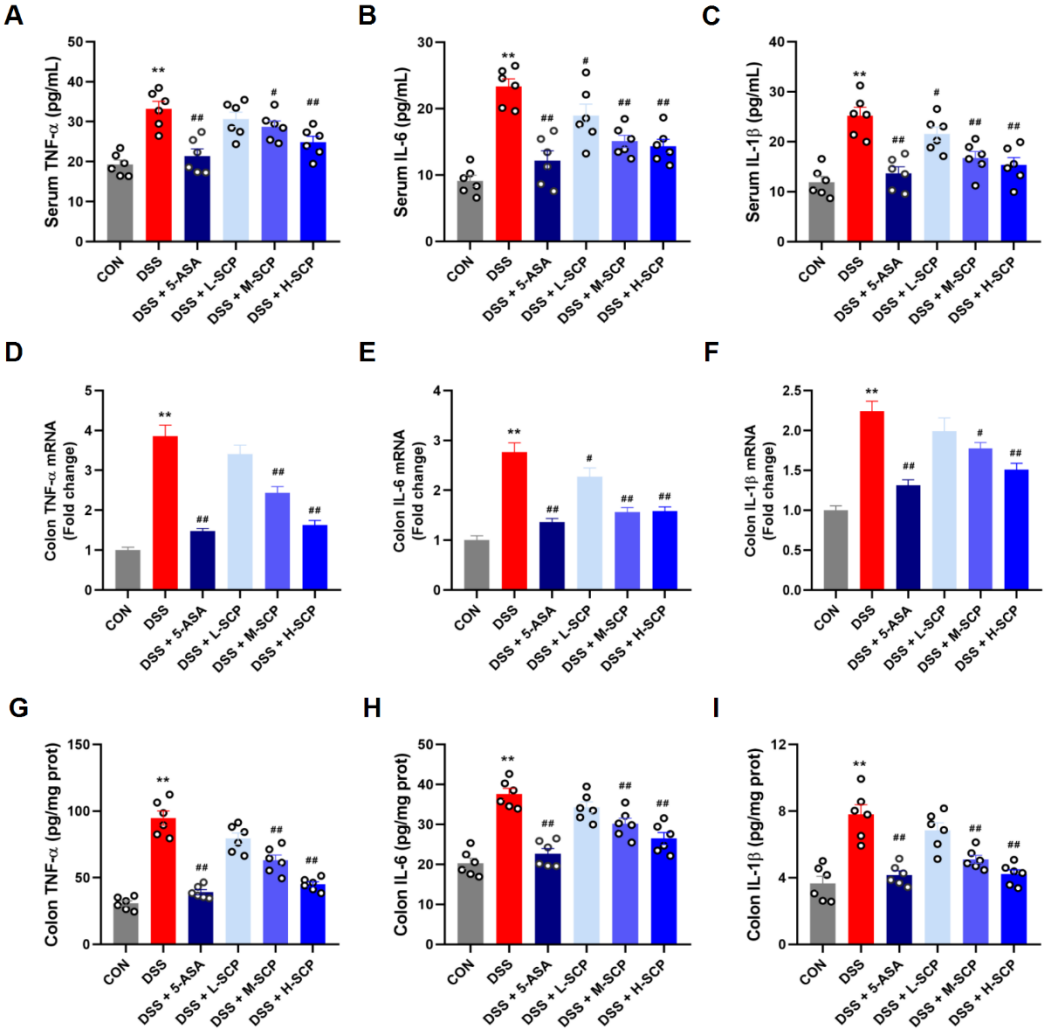

Figure 4 Effect of SCP on the secretion of cytokines and the expression of related genes in DSS-treated mice. Serum inflammatory factors (A) TNF-α, (B) IL-6, (C) IL-1β level; Colon inflammatory factors (D) TNF-α, (E) IL-6, (F) IL-1β mRNA expression; Colon inflammatory factors (G) TNF-α, (H) IL-6, (I) IL-1β level. Data are expressed as means ± SEM; n=6 for each group. *P<0.05, **P<0.01 compared with CON group; #P<0.05, ##P<0.01 compare with DSS group.

The effect of SCP on antioxidant enzyme activities in serum and colon of DSS-treated mice: Oxidative stress is involved in the onset and development of UC, and antioxidant enzymes (such as T-AOC and SOD) contribute to alleviating the intestinal inflammatory response (Zhu *et al*., 2022). To evaluate the effects of SCP on oxidative stress in serum and colon, the content of MDA, DAO, SOD, and T-AOC was measured. As shown in Fig. 4, compared with the CON group, serum MDA (Fig. 5A) concentration was significantly increased (P<0.01) in the DSS group, which was significantly reversed (P<0.01) by SCP and 5-ASA supplementation. Meanwhile, compared with the CON group, serum SOD (Fig. 5B) and T-AOC (Fig. 5C) activities were significantly decreased (P<0.01) in the DSS group. In addition, compared with the CON group, colon DAO (Fig. 5D) activity and MDA (Fig. 5E) level were significantly increased (P<0.01) in the DSS group, which was significantly reversed (P<0.01) by SCP and 5-ASA supplementation. Also, colon SOD (Fig. 5F) activity was significantly decreased (P<0.01) in the DSS group, which was significantly reversed (P<0.01) by SCP and 5-ASA supplementation. These results suggested that SCP could effectively alleviate oxidative stress damage in the colonic tissues of colitis mice.

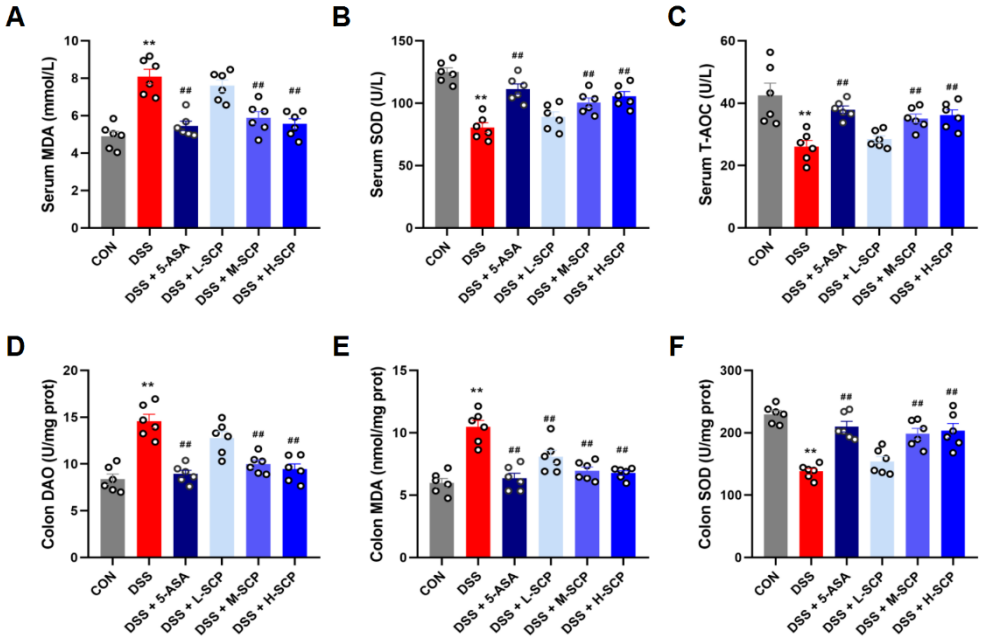

Figure 5 Effect of SCP on oxidative stress in DSS-induced mice. (A) Serum MDA level. (B) Serum SOD activity. (C) Serum T-AOC activity. (D) Colon DAO activity. (E) Colon MDA level. (F) Colon SOD activity. Data are expressed as means±SEM; n=6 for each group. $^{**}P<0.01$ compared with CON group; $^{\#\#}P<0.01$ compare with DSS group.

The effect of SCP on colon morphology and mucin content in DSS-treated mice: The histological changes of colon tissue were shown in Fig. 6. The result showed that DSS induced severe damage in colon tissues, such as loss of goblet cells and crypt structure, submucosal edema, and inflammatory cell infiltration. Compared with DSS group, the colon damage was significantly reduced ($P<0.01$) in the SCP or 5-ASA groups, including improved histological structure, more complete colitis mucosa epithelium, reduced epithelial disintegration, reduced inflammatory cell infiltration, and most goblet cells maintained normal physiological morphology (Fig. 6A). These results were further confirmed by histological scores (Fig. 6B). The number of colon goblet cells in DSS group was significantly lower ($P<0.01$) than that in CON. The number of goblet cells in SCP and 5-ASA groups was significantly recovered ($P<0.01$) as compared to the DSS group (Figs. 6C and 6D). These results suggested that SCP was effective in relieving acute colitis induced by DSS.

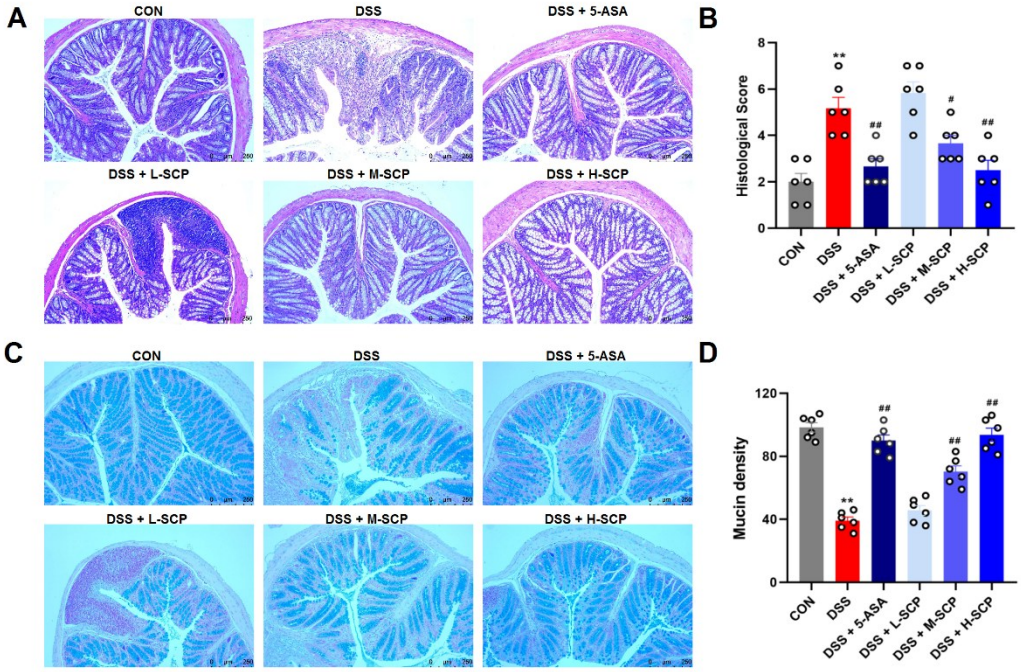

Figure 6 Effect of SCP on colon morphology in DSS-induced mice. (A) Representative H&E staining of colon tissues. (B) Histopathological scores of colons in each group. (C) AB-PAS staining. (D) Mucin density. Data are expressed as means ± SEM; n=6 for each group. $^{**}P<0.01$ compare with CON group; $^{\#}P<0.05$, $^{\#\#}P<0.01$ compare with DSS group.

The effect of SCP on colon tight junction proteins expression in DSS-treated mice: Impaired epithelial barrier function plays an important role in the pathogenesis of UC. To evaluate the protective effect of SCP on the intestinal barrier, the immunofluorescence staining was used to detect the expression of ZO-1 and occluding protein. The results showed that DSS intervention disrupted the epithelial barrier and significantly decreased (P<0.01) the mRNA and protein expression of ZO-1 (Figs. 7A, 7B, and 7C) and occludin (Figs. 7D, 7E, and 7F) as compared to the CON group. In contrast, SCP treatment significantly increased the expression of these proteins in colonic tissues as compared to the DSS group (Fig. 7).

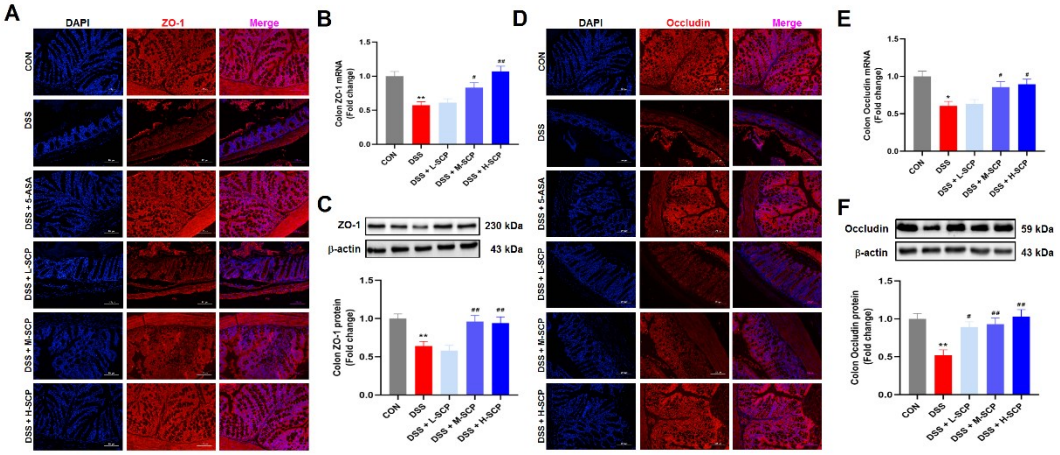

Figure 7 Effect of SCP on tight junction protein expression in colon of DSS-treated mice. (A) Immunofluorescence analysis of ZO-1 (n = 3). (B) Abundances of ZO-1 mRNA (n=6). (C) Content of ZO-1 protein (n = 3). (D) Immunofluorescence analysis of Occludin (n = 3). (E) Abundances of Occludin mRNA (n=6). (F) Content of ZO-1 protein (n = 3). Data are expressed as means ± SEM; n=6 for each group. *P<0.05, **P<0.01 compare with CON group; $^{\#}P$<0.05, $^{\#\#}P$<0.01 compare with DSS group.

The effect of SCP on TLR4/p65/IκBa pathway in the colon of DSS-treated mice: To further explore the mechanism of the mitigating effect of SCP on colon inflammation induced by DSS, the expression of TLR4/p65/IκBα pathway in the colon was detected. DSS markedly increased (P<0.001) the mRNA expression of TLR4 (Fig. 8A), p65 (Fig. 8B), and IκBα (Fig. 8C) in the colon. Meanwhile, it significantly increased (P<0.001) the protein content of TLR4 (Figs. 8D and E), p-p65/p65 (Figs. 8D and F), and p-IκBα/IκBα (Figs. 8D and G). However, SCP significantly (P<0.01) reversed the activation of TLR4/p65/IκBα pathway in a dose-dependent manner in the colon of DSS-treated mice.

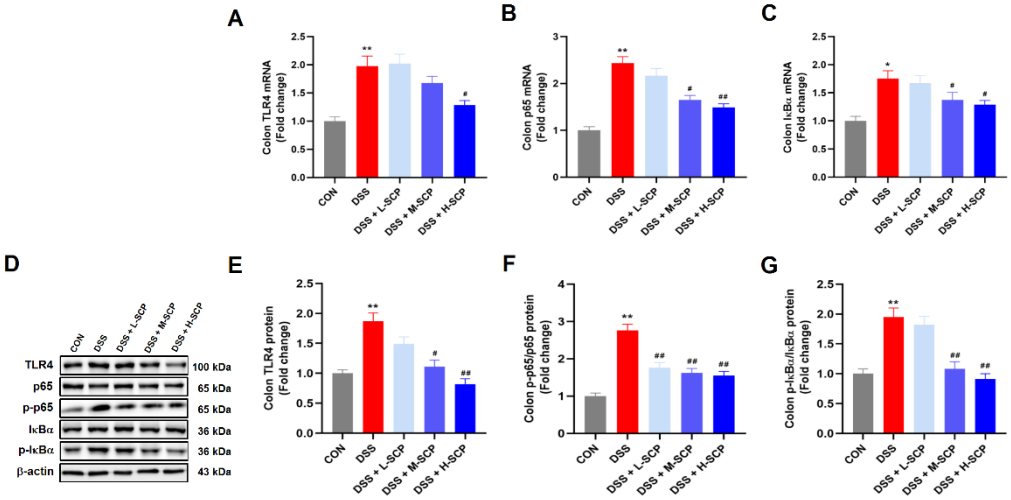

Figure 8 Effect of SCP on the expression of TLR4/p65/IκBα pathway in DSS-treated mice. (A) Abundances of TLR4 mRNA (n=6). (B) Abundances of p65 mRNA (n=6). (C) Abundances of IκBα mRNA (n=6). (D) Content of TLR4, p65, p-p65, IκBα and p-IκBα protein in Western blot analyses. (E) Content of TLR4 protein (n = 3). (F) Content of p-p65/p65 protein (n = 3). (G) Content of p-IκBα/IκBα protein (n = 3). Data are expressed as means ± SEM; n=6 for each group. *P<0.05, **P<0.01 compare with CON group; $^{\#}P$<0.05, $^{\#\#}P$<0.01 compare with DSS group.

The effect of SCP on intestinal microbial diversity in DSS-treated mice: To investigate the influence of DSS on the abundance of intestinal microbial, cecum microbiota was analyzed by 16S rRNA sequencing. Based on PCoA analysis, the abundance of microbial in the DSS group was clearly separated from other groups, while the DSS-SCP and 5-ASA group was closer to the CON group (Fig. 9A). In addition, LEfSe analysis indicated that *p_Firmicutes*, *o_Clostridiales*, *c_Clostridia*, *s_Lactobacillus_intestinalis*,

g_Anaerotruncus, *f_Clostridiaceae_1*, *g_Roseburia*, *g_Roseburia.s_uncultured_bacterium*, *g_Marvinbryantia*, and *g_Marvinbryantia.s_uncultured_bacterium* was highly expressed in the CON group. However, *p_Bacteroidetes*, *o_Bacteroidales*, *c_Bacteroidia*, *f_Bacteroidaceae*, *g_Bacteroides*, *s_Bacteroides_acidifaciens*, *s_Bacteroides_sartorii*, *s_Bacteroides_stercorirosoris*, *s_Bifidobacterium_animalis* and *s_Bacteroides_uniformis* were high abundance expression in DSS group. Whereas *f_Ruminococcaceae*, *g_Odoribacter.s_uncultured_bacterium*, *g_Odoribacter*, *g_Anaerovorax.s_uncultured_bacterium* and *s_Parabacteroides_distasonis* were high abundance expression in DSS_SCP group. And, *c_Bacilli*, *o_Lactobacillales*, *f_Lactobacillaceae*, *g_Lactobacillus*, *c_Actinobacteria*, *p_Actinobacteria*, *f_Bifidobacteriaceae*, *g_Bifidobacterium* and *o_Bifidobacteriales* were high abundance expression in 5-ASA group (Figs. 9B and 9C). According to alpha diversity analysis, DSS significantly (P<0.05) reduced the richness (Chao1 and Observed index) and Shannon index of cecum microbiota and increased the Simpson index. However, SCP markedly (P<0.05) reversed the change of alpha diversity index induced by DSS (Figs. 9D and 9I).

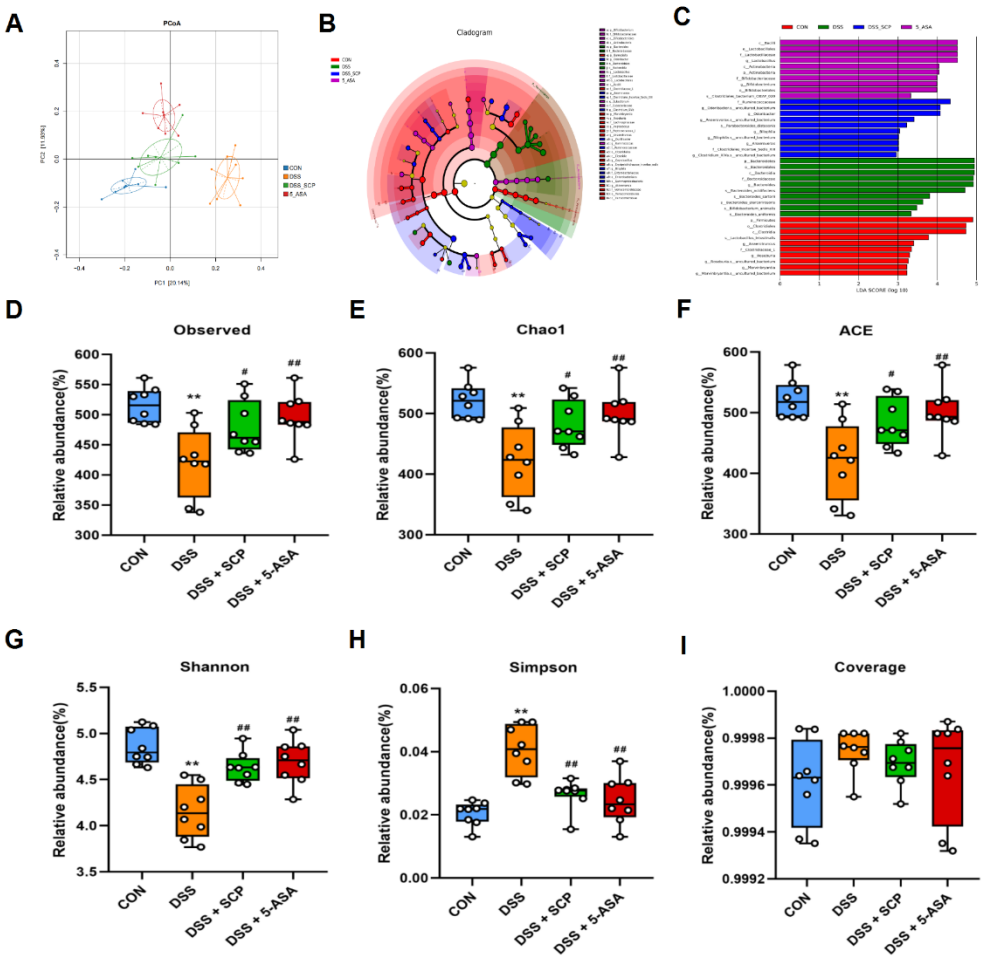

Figure 9 Effect of SCP on the composition of gut microbiota in DSS-treated mice. (A) PCoA of microbiota communities in the cecum. (B) LEfSe multi-level tree map. (C) LDA analysis (log10 LDA > 2.0). (D) Observed index. (E) Chao 1 index. (F) ACE index. (G) Shannon index. (H) Simpson index. (I) Coverage index. Data are expressed as means ± SEM; n=6 for each group. **P<0.01 compare with CON group; #P<0.05, ##P<0.01 compare with DSS group.

The effect of SCP on the composition of gut microbiota and SCFA levels in DSS-treated mice: At the phylum level, DSS markedly (P<0.05) reduced the abundance of *Firmicutes* and *Verrucomicrobia*, while significantly (P<0.05) increasing *Bacteroidetes* and *Actinobacteria*. Interestingly, the abundance of *Firmicutes* and *Verrucomicrobia* was up-regulated (P<0.05) and *Bacteroidetes* and *Actinobacteria* were down-regulated (P<0.05) in SCP-treated mice (Figs. 10A, 10B, 10C, 10D, 10E, 11A, and 11B). At the genus level, SCP markedly (P<0.05) reversed the decrease of *Lactobacillus*, *Akkermansia*, *Anaerobacterium*, and *Ruminococcus* relative abundance induced by DSS, as well as reversed (P<0.05) the increase of *Bacteroides* and *Intestinimonas* induced by DSS (Figs. 10F, 10G, 10H, 10I, 10J, 10K, 10L, 11C, and 11D). In addition, compared with CON group, the level of acetic acid, propionic acid, butyric acid, isobutyric acid, valeric acid were significantly decreased in DSS group, which was significantly reversed by SCP and 5-ASA supplementation (Fig. 12). Furthermore, the correlation between the key gut bacteria altered by SCP and inflammation, antioxidant related enzyme activity and SCFA was further analyzed Spearman correlation analysis. At the phylum level, Firmicutes was significantly (P<0.05) enhanced by SCP, were positively correlated with body weight, the levels of SOD, TP, ALB and T-AOC in serum, acetic acid, propionic acid, butyric acid and valeric acid in cecal contents, SOD in colon, while negatively correlated with the levels of AST, LDH in

serum, DAO in colon, MDA, TNF-α, IL-6 and IL-1β in serum and colon (Fig. 13A). In contrary, *Bacteroidetes* was significantly (P<0.05) decreased by SCP, were positively correlated with body weight, the levels of SOD, TP, ALB and T-AOC in serum, acetic acid, propionic acid, butyric acid and valeric acid in cecal contents, SOD in colon, while negatively correlated with the levels of AST, LDH in serum, DAO in colon, MDA, TNF-α, IL-6 and IL-1β in serum and colon (Fig. 13A). Similarly, at the genus level, the correlation between the relative abundance of *Lactobacillus*, *Anaerotruncus*, *Bacteroides* and inflammation, antioxidant related enzyme activity and SCFA present the same pattern with phylum level (Fig. 13B).

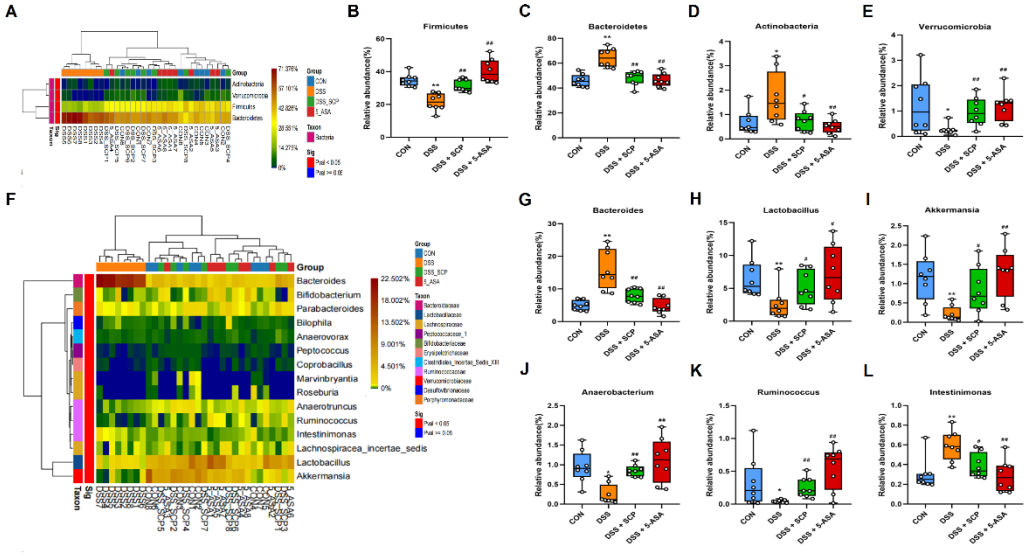

Figure 10 Effect of SCP on the composition of gut microbiota in DSS-treated mice. (A) Heatmap of the differential abundance of gut microbiota at the phylum level. The colors in the figure represent the relative abundance of the species, with a gradient from blue to red indicating the relative abundance of the species from small to large; (B) The relative abundance of *Firmicutes*; (C) The relative abundance of *Bacteroidetes*; (D) The relative abundance of *Actinobacteria*; (E) The relative abundance of *Verrucomicrobia*; (F) Heatmap of the differential abundance of gut microbiota at the genus level. (G) The relative abundance of *Bacteroides*; (H) The relative abundance of *Lactobacillus*; (I) The relative abundance of *Akkermansia*; (J) The relative abundance of *Anaerobacterium*; (K) The relative abundance of *Ruminococcus*; (L) The relative abundance of *Intestinimonas*. Data are expressed as means ± SEM; n=6 for each group. **P*<0.05, ***P*<0.01 compare with CON group; #*P*<0.05, ##*P*<0.01 compare with DSS group.

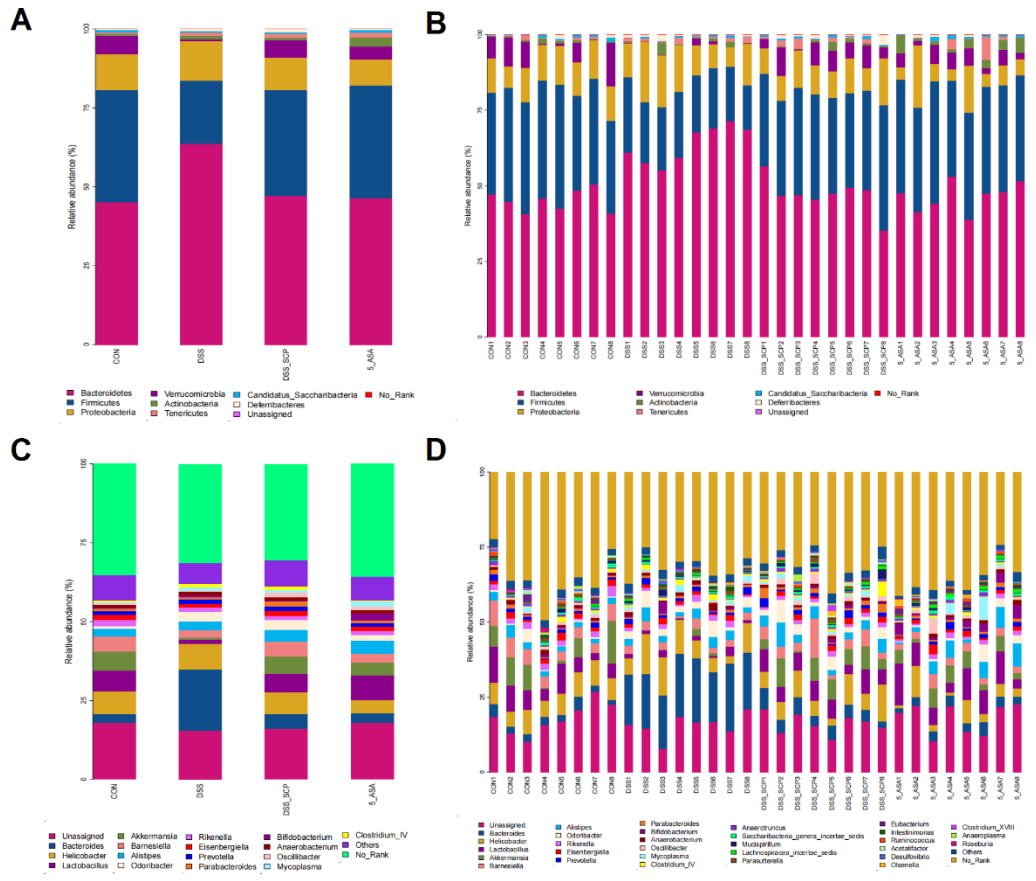

Figure 11 The relative abundance of cecal microbiota at the phylum and genus levels.

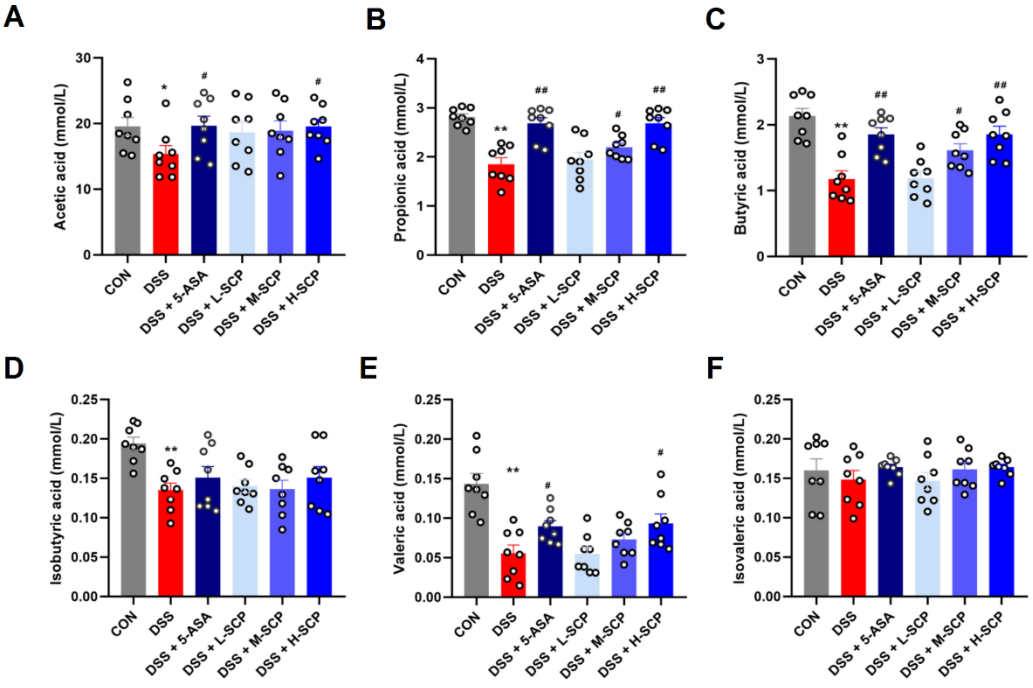

Figure 12 Effect of SCP on SCFA level in DSS-treated mice. (A) Acetic acid level. (B) Propionic acid level. (C) Butyric acid level. (D) Isobutyric acid level. (E) Valeric acid level. (F) Isovaleric acid level. Data are expressed as means ± SEM; n=6 for each group. **P*<0.05, ***P*<0.01 compare with CON group; #*P*<0.05, ##*P*<0.01 compare with DSS group.

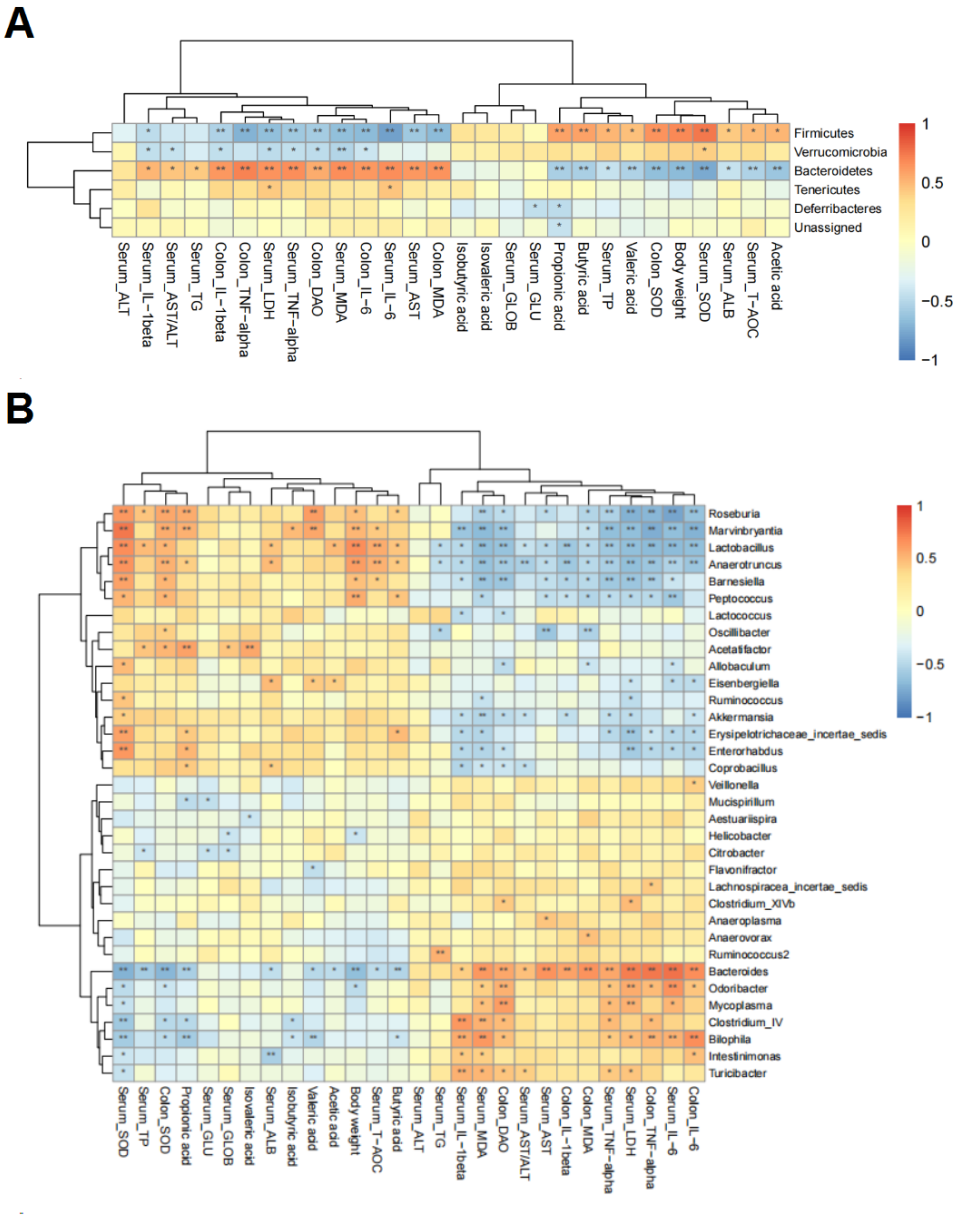

Figure 13 Correlation analysis between microbial abundance at the phylum and genus levels and environmental factors.

Discussion

Colitis is not only common but also experiencing an increasing prevalence worldwide, and it has become an increasingly common condition. Colitis is clinically characterized by prominent gastrointestinal symptoms, namely diarrhea, abdominal pain, and bloating. Pathologically, there are distinct changes within the colon, such as colon shortening, mucosal inflammation, crypt architectural distortion, and significant alterations in the gut microbiota composition. Many scholars are actively exploring treatment plans to alleviate colitis symptoms, including dietary adjustments, maintaining water-electrolyte balance, and traditional drug therapies. Among them, the application of natural substances such as polysaccharides in alleviating colitis symptoms has received significant attention. In the present study, we report for the first time the protective effect of polysaccharide from *Schisandra chinensis* (SCP) on DSS-induced colitis in mice. The monosaccharide composition analysis revealed that our SCP preparation is rich in glucose (45.91%), glucuronic acid (25.04%), and arabinose (11.96%). It is worth noting that the biological activity of polysaccharides is largely determined by their constituent monosaccharides and glycosidic linkages (Bian *et al*., 2022; Mukherjee *et al*., 2022). The high content of glucuronic acid, an acidic monosaccharide, is frequently associated with significant anti-inflammatory and immunoregulatory capacities (Liu *et al*., 2020; Mei *et al*., 2022). Polysaccharides containing glucuronic acid have been reported to enhance the intestinal barrier function and mitigate inflammatory responses by modulating key signaling pathways such as NF-κB (Mei *et al*., 2022; Xue *et al*., 2023). Similarly, arabinose-rich polysaccharides often exhibit potent antioxidant activities (Yang *et al*., 2023b). Therefore, the unique monosaccharide profile of SCP, characterized by a high proportion of glucuronic acid and arabinose, likely serves as a fundamental material basis for its observed efficacy in alleviating oxidative stress and inflammation in DSS-

induced colitis (Su *et al*., 2020; Bian *et al*., 2022). Similar studies have shown the positive impacts of polysaccharides obtained from different sources, such as *Armillariella tabescens* (Yang *et al*., 2023a) and *Hericium erinaceus* (Ren *et al*., 2023), on alleviating colitis symptoms. These studies, in combination with our current work, jointly underscore the crucial role of polysaccharides as potential therapeutic candidates for colitis, highlighting their structural diversity and functional versatility derived from natural sources.

In this study, our findings align with previous research that has shown the ability of polysaccharides to modulate antioxidant enzymes and inflammatory factors in colitis. DSS-exposed mice showed enhanced serum and colon inflammatory factors, such as TNF-α, IL-6, and IL-1β, which were reversed by treatment with SCP. This finding was consistent with previous studies reporting that SCP alleviated the increased ileum and colon TNF-α, IL-6, and IL-1β levels in antibiotic-associated diarrhea rats (Qi *et al*., 2019). This suggests that SCP can suppress inflammation and attenuate colitis severity. MDA levels are a key marker of oxidative damage in the serum and colon. In this study, we found that DSS exposure significantly increased MDA and DAO levels and inhibited SOD and T-AOC activities in the serum and colon of mice. However, treatment with SCP was effective in down-regulating MDA levels and up-regulating SOD and T-AOC activities. These findings indicate that SCP exerts antioxidant effects, which may contribute to its protective role against colitis-induced oxidative stress.

In addition, the activation of the TLR4/p65/IκBα pathway has been reported to be involved in DSS-induced colon inflammation in mice (Yan *et al*., 2023). Consistent with previous studies, we also found that both acute and chronic exposure to DSS led to the activation of the TLR4/p65/IκBα pathway in the colon of mice. Interestingly, SCP markedly inhibited the TLR4/p65/IκBα pathway in the colon induced by DSS. These results indicated that the TLR4/p65/IκBα pathway may mediate the protective effect of SCP on DSS-induced colon inflammation.

It was reported that DSS induced intestinal barrier damage by disrupting the tight junction proteins (Hu *et al*., 2023). SCP markedly up-regulated the expression of tight junction proteins (e.g., ZO-1 and Occludin) in the colon of DSS-exposed mice. These results suggest that SCP could assume the role of an anti-inflammatory therapy by sustaining the integrity of the intestinal mucosal barrier. Moreover, gut microbiota has been reported to play a critical role in regulating colitis (An *et al*., 2023). The Chao1, Observed, and Shannon diversity indices by OTU analysis indicated that DSS exposure markedly decreased the diversity and richness in cecum microbiota, whereas SCP supplementation reversed these differences. Consistent with our results, SCP administration reversed the decreased alpha diversity in antibiotic-associated diarrhea rats (Qi *et al*., 2019). At the phylum level, DSS exposure increased the abundance of *Bacteroidetes* and *Actinobacteria*, and reduced *Firmicutes* and *Verrucomicrobia*, while the changes were reversed by SCP administration. Similarly, Qi *et al*. (2019) reported that SCP markedly reversed the increase in *Bacteroidetes* and decrease in Firmicutes in antibiotic-associated diarrhea rats. Also, Yang *et al*. (2023a) reported that DSS exposure increased the abundance of *Bacteroidetes* and reduced *Firmicutes* abundance in mice. In addition, *Verrucomicrobia* has been reported to be involved in nutrient metabolism regulation and exert beneficial effects (Shuoker *et al*., 2023). The abundance of *Verrucomicrobia* was markedly down-regulated in DSS-treated mice and was elevated by treatment with SCP. Consistent with our results, Bain *et al*. reported that *Schisandra chinensis* extract markedly reversed the increase of *Verrucomicrobia* in DSS-induced mice (Bian *et al*., 2023). At the genus level, DSS exposure reduced the abundance of *Lactobacillus* and *Akkermansia* in mice. Most *Lactobacillus* species are probiotic microorganisms that produce enzymes with anti-biotic, anti-cancer, and immunosuppressant properties (Maria Remes Troche *et al*., 2020). Recent studies have found that *Akkermansia muciniphila*, a next-generation probiotic, plays a crucial role in improving host metabolic health and maintaining intestinal homeostasis (Jian *et al*., 2023). *Akkermansia* has been reported to improve obesity, inflammation, neurodegenerative diseases, and cancer through the gut-liver axis and gut-brain axis (Cani *et al*., 2022). Interestingly, in our study, SCP supplementation markedly enhanced the relative abundance of *Lactobacillus* and *Akkermansia* in DSS-treated mice. Altogether, based on these results, we infer that the gut microbiota, especially *Lactobacillus* and *Akkermansia*, contribute to the protective effect of SCP on colon inflammation in DSS-treated mice.

In conclusion, this study, SCP, a novel polysaccharide with a molecular weight (Mw) of 32.401 kDa, was extracted from the *Schisandra chinensis*. Our study provides evidence that SCP can alleviate DSS-induced colitis by improving intestinal microbiota abundance and inhibiting the TLR4/p65 pathway. The regulatory effects of SCP on body weight and colon inflammation may be ascribed to several factors. Firstly, SCP alleviated DSS-induced intestinal injury and oxidative stress. Secondly, SCP downregulated the expression of inflammatory factors and inhibited the TLR4/p65/IκBα pathway in the colon. Thirdly, SCP reversed DSS-induced intestinal barrier damage by improving the tight junction proteins. Finally, SCP improved the composition of gut microbiota, increased the diversity of gut microbiota, and the abundance of beneficial bacteria, especially *Lactobacillus* and *Akkermansia*. Nevertheless, the in-depth mechanism of *Lactobacillus* and *Akkermansia* in regulating colitis needs further evaluation.

Conflicts of interest: The authors declare no competing financial interests or personal relationships.

Acknowledgements

The experiment was supported by the Taizhou Science and Technology Support Programs (Agricultural Projects, TN202119), Jiangsu Agri-animal Husbandry Vocational Project (NSF2023ZR01), Jiangsu Provincial"Qing Lan" Project (2025).

Authors' contribution: Hui Lu analyzed and summarized the background information. Caihong

Wu, Yang Yang, and Peng Liu were the major contributors to writing the manuscript. All the authors participated in the design and conduct of the trial and approved the final manuscript.

Abbreviations: 5-ASA: 5-aminosalicylic acid; ALB: Albumin; DAI: Disease Activity Index; DAO, Diamine oxidase; DSS: dextran sulfate sodium; GLOB: Globulin; Glu: Glucose;IL-6, Interleukin-6; IL-1β, Interleukin-1β; LDH, Lactic dehydrogenase; MDA, Malondialdehyde; Mn, number molar masses; Mw, molecular weight; SCP, *Schisandra chinensis* polysaccharides SOD, Superoxide dismutase; T-AOC, Total antioxidant capacity; TG: Triglyceride; TNF-α, Tumor necrosis factor α; TP: Total protein.

References

An Y, Zhai Z, Wang X, Ding Y, He L, Li L, Mo Q, Mu C, Xie R, Liu T, Zhong W, Wang B and Cao H 2023. Targeting Desulfovibrio vulgaris flagellin-induced NAIP/NLRC4 inflammasome activation in macrophages attenuates ulcerative colitis. J Adv Res. 61: 63–75.

Bian Z, Qin Y, Li L, Su L, Fei C, Li Y, Hu M, Chen X, Zhang W, Mao C, Yuan X, Lu T and Ji D 2022. *Schisandra chinensis* (Turcz.) Baill. protects against DSS-induced colitis in mice: Involvement of TLR4/NF-κB/NLRP3 inflammasome pathway and gut microbiota. J Ethnopharmacol. 298: 115570.

Cani PD, Depommier C, Derrien M, Everard A and de Vos WM 2022. *Akkermansia muciniphila:* paradigm for next-generation beneficial microorganisms. Nat Rev Gastroenterol Hepatol. 19: 625–637.

Fu J, Li J, Sun Y, Liu S, Song F and Liu Z 2023. In-depth investigation of the mechanisms of Schisandra chinensis polysaccharide mitigating Alzheimer's disease rat via gut microbiota and feces metabolomics. Int J Biol Macromol. 232: 123488.

Glorieux G, Nigam SK, Vanholder R and Verbeke F 2023. Role of the microbiome in gut-heart-kidney cross talk. Circ Res. 132: 1064–1083.

Gobert AP, Latour YL, Asim M, Barry DP, Allaman MM, Finley JL, Smith TM, McNamara KM, Singh K, Sierra JC, Delgado AG, Luis PB, Schneider C, Washington MK, Piazuelo MB, Zhao S, Coburn LA and Wilson KT 2022. Protective role of spermidine in colitis and colon carcinogenesis. Gastroenterology 162: 813–827.

Hu Y, He Z, Zhang J, Zhang C, Wang Y, Zhang W, Zhang F, Gu F and Hu W 2023. Effect of Piper nigrum essential oil in dextran sulfate sodium (DSS)-induced colitis and its potential mechanisms. Phytomedicine 119: 155024.

Jian H, Liu Y, Wang X, Dong X and Zou X 2023. Akkermansia muciniphila as a next-generation probiotic in modulating human metabolic homeostasis and disease progression: A role mediated by gut-liver-brain axes? Int J Mol Sci. 24.

Kobayashi T, Siegmund B, Le Berre C, Wei SC, Ferrante M, Shen B, Bernstein CN, Danese S, Peyrin-Biroulet L and Hibi T 2020. Ulcerative colitis. Nat Rev Dis Primers. 6: 74.

Li Z, He X, Liu F, Wang J and Feng J 2018. A review of polysaccharides from Schisandra chinensis and Schisandra sphenanthera: Properties, functions and applications. Carbohydr Polym. 184: 178–190.

Liu X, Liu D, Chen Y, Zhong R, Gao L, Yang C, Ai C, El-Seedi HR and Zhao C 2020. Physicochemical characterization of a polysaccharide from Agrocybe aegirita and its anti-ageing activity. Carbohydr Polym. 236: 116056.

Liu Y, Zhang H, Xie A, Sun J, Yang H, Li J, Li Y, Chen F, Mei Y and Liang Y 2023. *Lactobacillus rhamnosus* and L. plantarum combination treatment ameliorated colitis symptoms in a mouse model by altering intestinal microbial composition and suppressing inflammatory response. Mol Nutr Food Res. 67: e2200340.

Lu H, Shen M, Chen Y, Yu Q, Chen T and Xie J 2023. Alleviative effects of natural plant polysaccharides against DSS-induced ulcerative colitis via inhibiting inflammation and modulating gut microbiota. Food Res Int. 167: 112630.

Maria Remes Troche J, Coss Adame E, Valdovinos Diaz MA, Gomez Escudero O, Icaza Chavez ME, Chavez-Barrera JA, Zarate Mondragon F, Ruiz Velarde Velasco JA, Aceves Tavares GR, Lira Pedrin MA, Cerda Contreras E, Carmona Sanchez RI, Guerra Lopez H and Solana Ortiz R 2020. *Lactobacillus acidophilus* LB: A useful pharmabiotic for the treatment of digestive disorders. Ther Adv Gastroenterol. 13: 1756284820971201.

Mei Z, Huang X, Zhang H, Cheng D, Xu X, Fang M, Hu J, Liu Y, Liang Y and Mei Y 2022. Chitin derivatives ameliorate DSS-induced ulcerative colitis by changing gut microbiota and restoring intestinal barrier function. Int J Biol Macromol. 202: 375–387.

Mukherjee S, Jana S, Khawas S, Kicuntod J, Marschall M, Ray B and Ray S 2022. Synthesis, molecular features and biological activities of modified plant polysaccharides. Carbohydr Polym. 289: 119299.

Qi Y, Chen L, Gao K, Shao Z, Huo X, Hua M, Liu S, Sun Y and Li S 2019. Effects of Schisandra chinensis polysaccharides on rats with antibiotic-associated diarrhea. Int J Biol Macromol. 124: 627–634.

Ren Y, Sun Q, Gao R, Sheng Y, Guan T, Li W, Zhou L, Liu C, Li H, Lu Z, Yu L, Shi J, Xu Z, Xue Y and Geng Y 2023. Low weight polysaccharide of Hericium erinaceus ameliorates colitis via inhibiting the NLRP3 inflammasome activation in association with gut microbiota modulation. Nutrients 15: 739.

Schlegel N, Boerner K and Waschke J 2021. Targeting desmosomal adhesion and signalling for intestinal barrier stabilization in inflammatory bowel diseases—Lessons from experimental models and patients. Acta Physiol. 231: e13492.

Shi J, Wang Y, Cheng L, Wang J and Raghavan V 2022. Gut microbiome modulation by probiotics, prebiotics, synbiotics and postbiotics: a novel strategy in food allergy prevention and treatment. Crit Rev Food Sci Nutr. 1–17.

Shi L, Fang B, Yong Y, Li X, Gong D, Li J, Yu T, Gooneratne R, Gao Z, Li S and Ju X 2019. Chitosan oligosaccharide-mediated attenuation of LPS-induced inflammation in IPEC-J2 cells is related to the TLR4/NF-κB signaling pathway. Carbohydr Polym. 219: 269–279.

Shuoker B, Pichler MJ, Jin C, Sakanaka H, Wu H, Gascuena AM, Liu J, Nielsen TS, Holgersson J,

Nordberg Karlsson E, Juge N, Meier S, Morth JP, Karlsson NG and Abou Hachem M 2023. Sialidases and fucosidases of Akkermansia muciniphila are crucial for growth on mucin and nutrient sharing with mucus-associated gut bacteria. Nat Commun. 14: 1833.

Sinha SR, Haileselassie Y, Nguyen LP, Tropini C, Wang M, Becker LS, Sim D, Jarr K, Spear ET, Singh G, Namkoong H, Bittinger K, Fischbach MA, Sonnenburg JL and Habtezion A 2020. Dysbiosis-induced secondary bile acid deficiency promotes intestinal inflammation. Cell Host Microbe. 27: 659–670.

Spencer J and Bemark M 2023. Human intestinal B cells in inflammatory diseases. Nat Rev Gastroenterol Hepatol. 20: 254–265.

Su L, Mao C, Wang X, Li L, Tong H, Mao J, Ji D, Lu T, Hao M, Huang Z, Fei C, Zhang K and Yan G 2020. The anti-colitis effect of Schisandra chinensis polysaccharide is associated with the regulation of the composition and metabolism of gut microbiota. Front Cell Infect Microbiol. 10: 519479.

Wang T, Han J, Dai H, Sun J, Ren J, Wang W, Qiao S, Liu C, Sun L, Liu S, Li D, Wei S and Liu H 2022. Polysaccharides from Lyophyllum decastes reduce obesity by altering gut microbiota and increasing energy expenditure. Carbohydr Polym. 295: 119862.

Wen XD, Wang CZ, Yu C, Zhang Z, Calway T, Wang Y, Li P and Yuan CS 2013. Salvia miltiorrhiza (dan shen) significantly ameliorates colon inflammation in dextran sulfate sodium-induced colitis. Am J Chin Med. 41: 1097–1108.

Wu F, Wuri G, Fang B, Shi M, Zhang M and Zhao L 2023. Alleviative mechanism and effect of Bifidobacterium animalis A6 on dextran sodium sulfate-induced ulcerative colitis in mice. Food Sci Nutr. 11: 892–902.

Xiao F, Dong F, Li X, Li Y, Yu G, Liu Z, Wang Y and Zhang T 2022. Bifidobacterium longum CECT 7894 improves the efficacy of infliximab for DSS-induced colitis via regulating the gut microbiota and bile acid metabolism. Front Pharmacol. 13: 902337.

Xue G, Xiong H, Wang S, Fu Y and Xie Y 2023. Eudragit-coated chitosan-tripterygium glycoside conjugate microspheres alleviate DSS-induced experimental colitis by inhibiting the TLR4/NF-κB signaling pathway. Biomed Pharmacother. 158: 114194.

Yan B, Li X, Zhou L, Qiao Y, Wu J, Zha L, Liu P, Peng S, Wu B, Yu X and Shen L 2022. Inhibition of IRAK1/4 alleviates colitis by inhibiting TLR4/NF-κB pathway and protecting the intestinal barrier. Bosn J Basic Med Sci. 22: 872–881.

Yang R, Wang Y, Mehmood S, Zhao M, Yang X, Li Y, Wang W, Chen J and Jia Q 2023a. Polysaccharides from Armillariella tabescens mycelia mitigate DSS-induced ulcerative colitis via modulating intestinal microbiota in mice. Int J Biol Macromol. 245: 125538.

Yang Y, Jiang W, Feng Y, Liu J, Chen H, Wang D and Zhao R 2021. Melatonin alleviates hippocampal GR inhibition and depression-like behavior induced by constant light exposure in mice. Ecotoxicol Environ Saf. 228: 112979.

Yang Y, Yu L, Zhu T, Xu S, He J, Mao N, Liu Z and Wang D 2023b. Neuroprotective effects of Lycium barbarum polysaccharide on light-induced oxidative stress and mitochondrial damage via the Nrf2/HO-1 pathway in mouse hippocampal neurons. Int J Biol Macromol. 251: 126315.

Zhang Q, Wang L, Wang S, Cheng H, Xu L, Pei G, Wang Y, Fu C, Jiang Y, He C and Wei Q 2022. Signaling pathways and targeted therapy for myocardial infarction. Signal Transduct Target Ther. 7: 78.

Zhu YY, Thakur K, Feng JY, Zhang JG, Hu F, Cespedes-Acuña CL, Liao C and ZJ 2022. Riboflavin bioenriched soymilk alleviates oxidative stress mediated liver injury, intestinal inflammation, and gut microbiota modification in B2 depletion–repletion mice. J Agric Food Chem. 70: 3818–3831.